Organic crystals – More than simple additives toward better electroceramic materials

Mamoru Senna[1,*], Chie Ando[2], Mirjana Vijatović Petrović[3], Jelena Bobić[3], Biljana Stojanović[3]

[1]*Faculty of Science and Technology, Keio University Hiyoshi, Yokohama 223-8522, Japan*
[2]*Material Development Department, Taiyo Yuden Co., Ltd., Nakamuroda, Takasaki, 370-3347, Japan*
[3]*Center for Multidisciplinary Studies, University of Belgrade, Kneza Viseslava 1a, 11000 Beograd, Serbia*

Received 31 January 2010; received in revised form 25 May 2010; accepted 24 July 2010

Abstract

Roles of various organic crystals (OC), notably those containing nitrogen, on the preparation and properties of source materials for electroceramics are featured from the author's own experimental studies. When OC are intimately mixed with metal salts like carbonates, their decomposition is accelerated, liberating the diffusing species at temperatures lower than usual. Mixing of OC with metal oxides under mechanical stressing results in anion exchange and eases diffusion of guest species. Case studies on 3 categories, i.e. i) substitution of oxygen in titania with nitrogen and introduction of oxygen vacancies during co-grinding titania with urea, glycine and/or polytetra fluoroethylene; ii) increase in the rate of reaction of barium titanate formation via a solid state route by OCs with detailed process analysis with glycine as an example of OC, and iii) phase pure solid state synthesis of $Li_4Ti_5O_{12}$ by mechanically activating the intermediate, Li_2TiO_3 with 3 amino acids as OCs.

Keywords*: organic solids, mechanical stressing, ligand exchange, anion substitution, oxygen vacancy*

I. Introduction

Among many aspects of organic additives in ceramic processing, starting from traditional surface modification, surfactants, dispersing aids, coordination of organic compounds with lone pair electrons play a unique role on the preparation of better electroceramic materials. Coordination reaction can occur in a solid state process by using organic crystals (OC).

Properties of OC are categorically different from those of conventional inorganic crystals. In OC, each lattice site is occupied by a molecule, so that they belong to a group of molecular crystals. They are generally much softer than conventional inorganic crystals, primarily because of the nature of the bonding among the species occupying the lattice points, i.e. based either on the van der Waals force or on the hydrogen bonding [1–3]. Smaller densities associated with the light atoms and oriented bondings are also contributing the softness of OCs. As a consequence, OCs are prone to deform themselves much more easily under mechanical stressing [4–7], as compared to conventional inorganic crystals like metal oxides. The consequence of crystal deformation is also very different between organic and inorganic crystals. While deformation of crystal- or ligand fields are of primary importance for inorganic crystals, both inter- and intramolecular energy states change in OC, due to changes in the large number of interatomic distances involved in OC [8,9]. The latter change is inevitably associated with the change in the local electron distribution. This, in turn, brings about symmetry loss of each ingredient molecule and, hence, increases the local polarity [10]. This further triggers charge transfer across the boundary between dissimilar particles. Cross boundary charge transfer often initiates formation of bridging bonds between the counterparts of the mixture [11].

When a mixture of inorganic and organic crystals is mechanically stressed, deformation of a ligand field of inorganic crystals takes place in the presence of deformed organic crystals with deformed molecules. This leads to various unconventional phenomena like ligand exchange [12,13].

* Corresponding author: tel: +81 42 483 4538
fax: +81 42 483 4538, e-mail: *senna@applc.keio.ac.jp*

In the present feature article, the authors try to summarize their own works in the related topics, in an attempt to find out some common basics of electroceramic synthesis via a solid state route. Some case studies are reviewed, including anion exchange of titania at room temperature and low temperature synthesis of perovskite compounds.

II. Modification of TiO_2 by OC

2.1 Role of titania on the electroceramic syntheses

Titania is one of the most important starting materials for electroceramic materials. In solid state processes during the preparation of titanate syntheses, it is usual that titania fine particles are involved in the starting reaction mixture. It is generally accepted that divalent ionic species are diffusing into a titania lattice during calcination [14–16]. It is therefore of particular importance to use titania as fine and as active as possible, in order to increase the rate of diffusion and to minimize the diffusion distance in order to complete the solid state reaction at temperatures as low as possible. Importance of low temperature synthesis cannot be overemphasized to adapt ever increasing needs for micronization of electronic devices. Some examples are given below, extracted from the author's latest experimental study.

2.2 Anion exchange of titania by co-grinding with organic crystals

When anatase fine particles were co-ground with OC, e.g. urea, glycine, or PTFE, the colourless starting materials are tinted, as recognized by representative diffuse reflectance spectra [17], shown in Fig. 1. The absorbance at around 420 nm, corresponding to yellowish colour for those with urea or glycine is an indication of partial substitution of oxygen with nitrogen [18]. A broad absorbance in the wide visible region was observed when PTFE was added to titania was also observed [17]. This is attributable to the introduction of two different species of oxygen vacancies with one and two trapped electrons and d-d transition of Ti^{3+}. The latter suggests partial reduction of the central Ti^{4+} ion in the structural units of titania, i.e., TiO_6 octahedra.

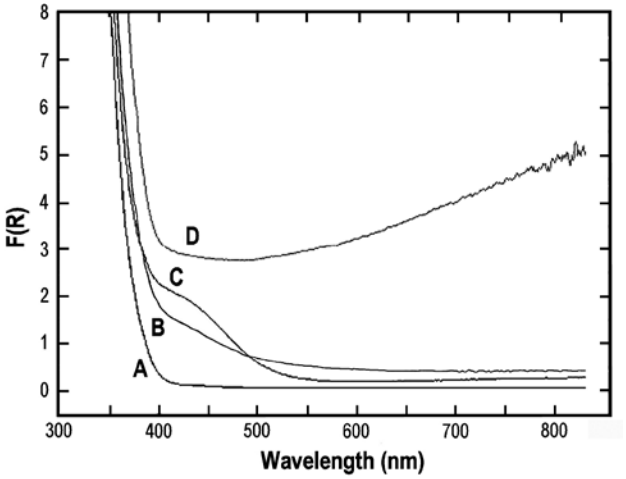

Figure 1. UV-Vis diffuse reflectance spectra. A: Intact titania, milled for 1 h. B, C and D: Titania + glycine, urea and PTFE, respectively

High-resolution TEM revealed selective amorphization at the near surface region, as shown in Fig. 2, although intense X-ray diffraction peaks survive even after prolonged co-grinding. Fragmentation of apparent primary particles was also observed. This parallels the downsizing of the coherent long range ordering units, i.e. crystallites. Near-surface amorphization as a consequence of mechanical stressing also happens even without additives [19,20], suggesting a possible symmetry loss of the TiO_6 units, merely by stressing, together with the disordering of the octahedra. It is important to recognize that nitrogen serves as an acceptor, N^{3-}, to replace a part of oxygen of titania [21]. On the other hand, N–O

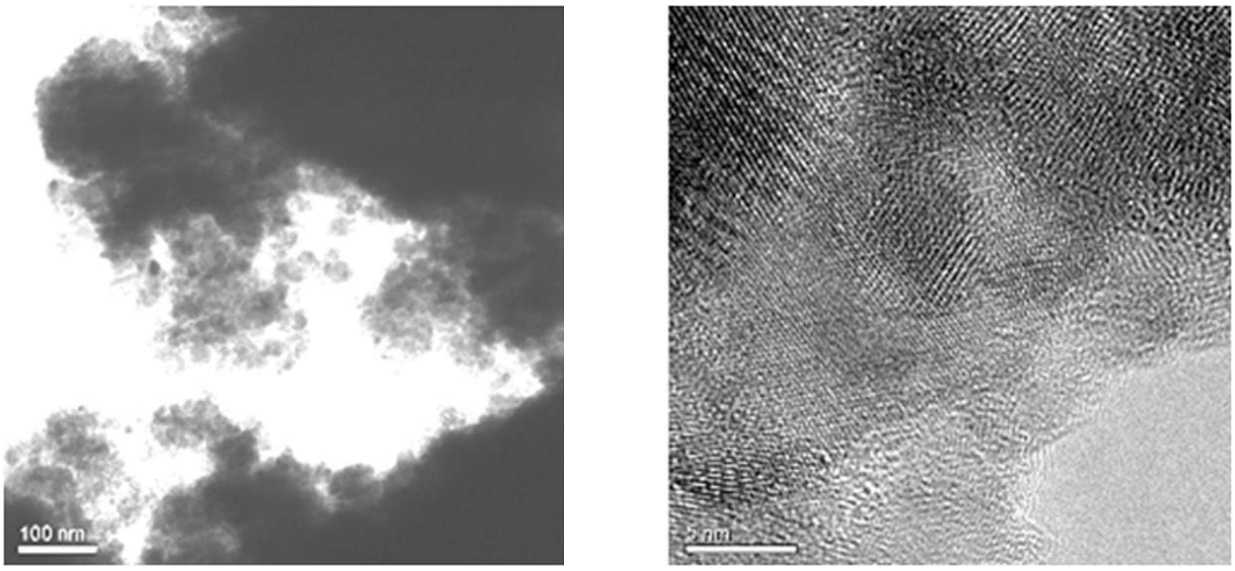

Figure 2. Transmission electron micrographs for the mixture, titania + PTFE + urea, milled for 3 h under two different magnifications

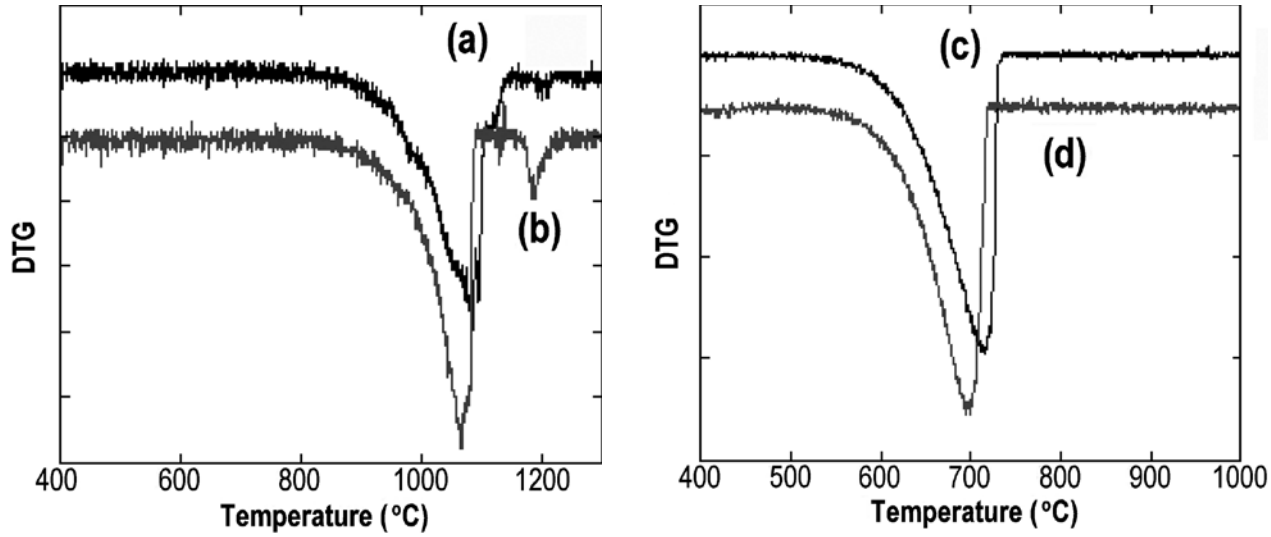

Figure 3. Differential thermogravimetry profiles for carbonates decomposition: (a) $BaCO_3$, (b) $BaCO_3$ with 0.4 wt.% nylon, (c) $CaCO_3$ and (d) $CaCO_3$ with 0.4 wt.% nylon

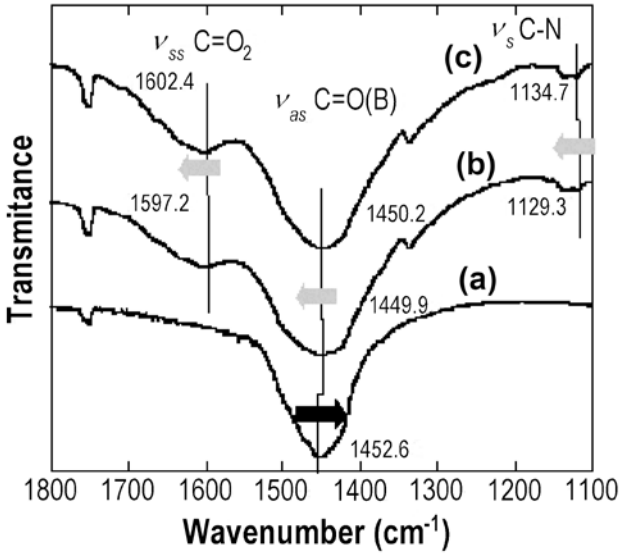

Figure 4 Chemical shift of IR spectra of $BaCO_3$ + TiO_2 (a) by adding glycine (b) and subsequently milling for 3 h (c)

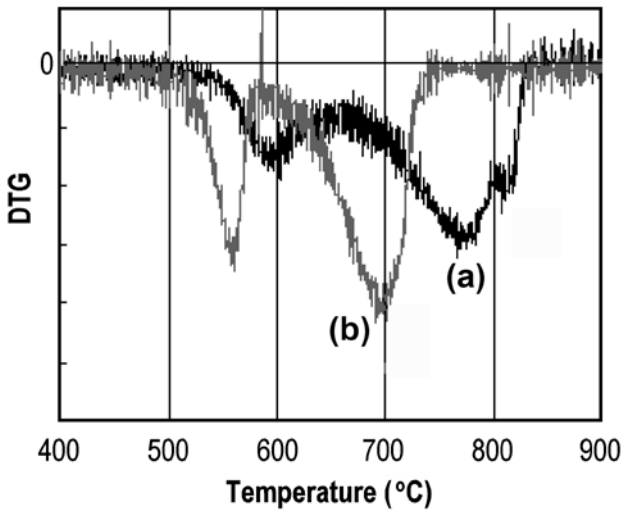

Figure 5. Differential thermogravimetry profiles for the mixture, $BaCO_3$, + TiO_2, intact (a) and by adding 1.5 wt.% glycine and milled for 1 h (b)

substitution introduces oxygen vacancies due to charge compensation [22]. This is enhanced when the contact point between titania and OC is subjected to mechanical stressing, just because of amorphization of the near-surface region, and forced contact as mentioned above.

All the associated phenomena, i.e. partial N–O substitution, introduction of oxygen vacancies, as well as partial reduction of the central titanium ion favour the ligand exchange around the central titanium ion, serving as a Lewis acid. Thus, a mechanochemical anion exchange reaction could be interpreted as a kind of autocatalytic processes. In other words, introduction of nitrogen and oxygen vacancies might be synergetic under mechanical stressing.

III. Effects of OC addition on the incipient solid state reaction for electroceramics

3.1 Reaction initiation at lower temperatures by OC

Change in the decomposition behaviour is one of the most remarkable effects of OC addition to the reaction mixture of electroceramics, as shown in Fig. 3, where the decomposition temperature of Ba and Ca carbonates are shown to decrease significantly by adding nylon powder. This was found by chance, as we suspected some chemical effects of ball milling with nylon coated steel balls [23]. This aspect is discussed in more detail later on.

Based on this experimental finding, we tried to apply some N– containing OC to the reaction mixture of barium titanate (BT) in the hope to reduce the temperature needed to BT formation by starting from a conventional reaction mixture, comprising $BaCO_3$ and TiO_2.

The mechanochemical effects of milling with the nylon-coated steel balls on the mixture, $BaCO_3$ and TiO_2, were found to be favourable without agglomeration [23]. Out of a number of possible effects of milling with nylon balls, we suspected some chemical effects of ny-

lon, as an amide compound as well. As a matter of fact, we have found a positive effect of adding a water-soluble protein, bovine serum albumin (BSA), and an amide bonded polymer like nylon, to obtain micro-particles of BT [24]. The principal role of these OCs is primarily the coordination of OCs to Ba, easing the decomposition of $BaCO_3$, as revealed by IR spectra shown in Fig. 4. Common factors among these additives are relatively stable solids with C=O and >NH bonds to coordinate as a ligand to Ba^{2+}. N-coordination was found to destabilize the counter-ion, CO_3^{2-}, to ease decomposition of $BaCO_3$ and, hence, decreases the calcination temperature [25]. Therefore, glycine (GLY), one of the simplest amino acids, was forced as a representative OC.

Addition of GLY to the ceramic precursor was often regarded as a fuel in a combustion process with nitrates to obtain fine starting powders [26]. The role of GLY to decrease the decomposition temperature of the starting material, to be discussed here is entirely different from the ideas of using GLY in ceramics processing as a fuel.

3.2 Effects of GLY on reaction processes of BT formation

The reaction between $BaCO_3$ and TiO_2 is primarily described as:

$$BaCO_3 + TiO_2 \rightarrow BaTiO_3 + CO_2\uparrow \qquad (1)$$

The reaction is accompanied by the CO_2 evolution, so that the reaction process is conveniently monitored by thermogravimetry. Representative differential thermogravimetry (DTG) profiles are illustrated in Fig. 5. Two important observations are: i) both of the DTG profiles are bimodal, and ii) the initiation temperature significantly decreases with the addition of an amino acid, glycine (GLY). Decrease in the initiation temperature is shown in Table 1.

The bimodality of DTG profiles shown in Fig. 5 cannot be explained by assuming a single reaction path of equation (1). Indeed, it is well known that not all the reaction goes simultaneously to an end, since the reaction front is restricted to the initial contact point between dissimilar particles, i.e. $BaCO_3$ and TiO_2.

The later stage of the reaction is predominated by the diffusion of Ba^{2+} toward TiO_2 through BT product [8], which is formally described as:

$$BaTiO_3 + BaCO_3 \rightarrow Ba_2TiO_4 + CO_2\uparrow \qquad (2)$$

Closer look at Fig. 5 reveals that the mixture without GLY (sample S) exhibits a larger portion of the first stage of the bimodal DTG profile.

The reaction process monitored by weight loss is closely related to those monitored by *ex situ* X-ray diffractometry, as shown in Fig. 6. This indicates that the decomposition of $BaCO_3$ is immediately followed by the quick nucleation-growth process of BT.

Table 1. Change in the reaction initiation temperature of barium titanate formation with the concentration of the additive, glycine

Glycin [wt.%]	Initial temperature [°C]
0	548
1.0	537
2.0	523
20.0	509

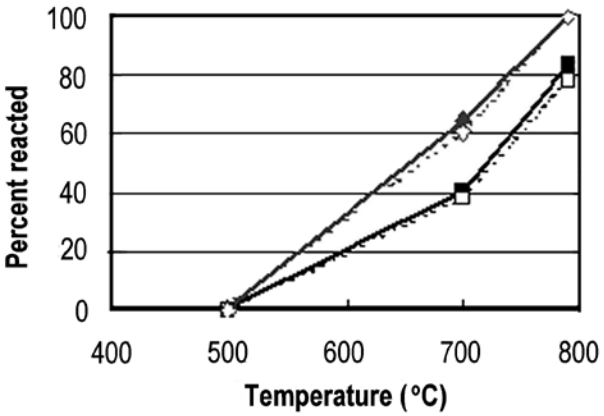

Figure 6. Relationship between percent-reaction and temperature reactions, determined by TG (broken line) and XRD (solid line) for the intact mixture (a) and after adding 1.5 wt.% glycine and milled for 1 h (b)

3.3 Relation between particle size and crystallinity of BT

Decrease in the initiation temperature of the reaction toward BT is straightforwardly associated with the possibility of low temperature synthesis of BT. This is particularly beneficial for microelectronic devices like multi-layered ceramic capacitor (MLCC). Toward this kind of technical development, however, the particle size should be kept as small as possible, while the crystallinity as high as possible. This is really challenging since increase in the crystallinity requires elimination of lattice imperfections. This is achieved by increasing in the atomic mobility in the lattice. The same driving force, however, serves to increase in the size of particles or grains as well. To surmount these seemingly contradicting hurdles, we have to go further to elucidate the mechanisms involved.

All the weight loss processes shown in Fig. 5 were terminated at temperatures below 800°C. Completion of the weight loss does not, however, imply the completion of BT synthesis for practical application, since we do need a good crystallinity. Prolonged annealing of the product at the temperature of weight loss completion, i.e. ca. 800°C is inadequate for the good crystallinity, evaluated by the tetragonality. With an increase in the calcination temperature, development of crystalline structure and grain growth occur simultaneously. We therefore need some tactic to favour a decrease in the lattice imperfection, while suppressing the grain growth. We have therefore to think at this

stage, whether and to what extent the difference between these processes exists.

For ferroelectric materials, of primary importance is their high dielectric constant value. In perovskite materials, the ratio of the lattice constants, *c/a*, called tetragonality, serve as the measure of high crystallinity. Phenomenologically, it is recognized that the smaller grains contain higher amount of lattice imperfections so that their tetragonality becomes smaller and approaches finally to unity, where the lattice turns cubic. When the tetragonality is plotted against the grain size, general tendency is a sharp drop of *c/a* when the grain size decreases to a critical value. For BT samples obtained from the reaction mixture with GLY, however, the values are found in the upper left area of the plot shown in Fig. 7, indicating exceptionally high value of the tetragonality in spite of the small grain size. This is very favourable for the application to MLCC.

3.4 Coalescence of BT after apparent reaction completion

Fig. 8 compares the morphology of the reaction products at 880°C, i.e. at temperature well above the termination of the weight loss [27]. Grains obtained from the mixture with GLY are more spherical. We further examined microstructural differences in the samples with and without GLY by comparing samples quenched from 700 and 790°C. As shown in Fig. 9 for those obtained from the samples quenched from 700°C, we observe two distinct particle groups, i.e. those above 100 nm and agglomerated ones of about 50 nm with very fine primary particles. With the aid of EDX analysis, we revealed that the larger ones are $BaCO_3$. Furthermore, we confirmed that titania agglomerates were surrounded by fine BT particles. These trends remained unchanged as we increased the heating temperature from 700 to 790°C. Remaining $BaCO_3$ particles grew up to increase the local compositional inhomogeneity, leading to a broader particle size distribution of BT, particularly in the case of sample without GLY.

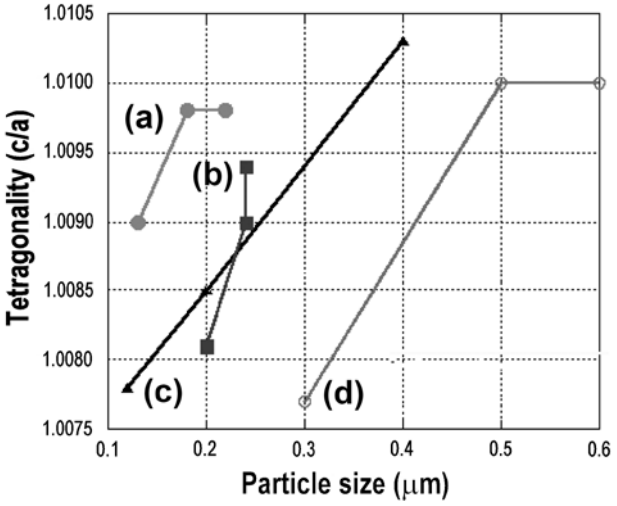

Figure 7. Relationship between tetragonality and particle size of barium titanate prepared from the reactant mixture (a) milled with 0.5 wt.% glycine for 3 h, (b) milled for 10 h, (c) the mixture, $BaCO_3$ + TiO_2, intact, and (d) from literature (T. Yamamoto et al, Jpn. J. Appl. Phys., 39 (2000) 5683)

The particle size distribution was obtained from those micrographs and shown in Fig. 10. We note that the average particle size of sample with GLY was twice larger than those without GLY. This implies that dry milling with GLY accelerates not only the BT formation but also BT particle growth simultaneously.

3.5 Behaviour of GLY during calcination

Chemical states of OC change when they are intimately mixed with inorganic substances like $BaCO_3$, TiO_2 or their mixture, due to various kinds of chemical interactions. This is reflected, for instance on the thermal behaviour [28]. As shown in Fig. 11, decomposition of intact GLY takes place at around 245°C, while those mixed with inorganic solids exhibit multimodal DTG and DTA profiles with their peak top temperature higher than those of intact GLY. The change in the DTG peak is more complicated, particularly for those at higher temperatures, depending on the states of in-

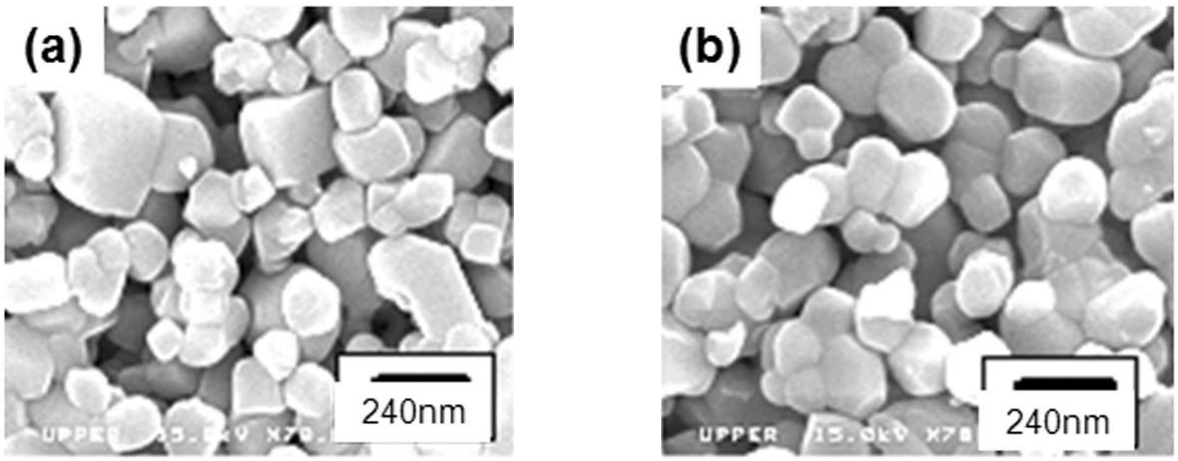

Figure 8. Grain morphology of barium titanate calcined at 880°C from: (a) intact mixture and (b) the mixture milled with 1.5 wt.% glycine for 1 h

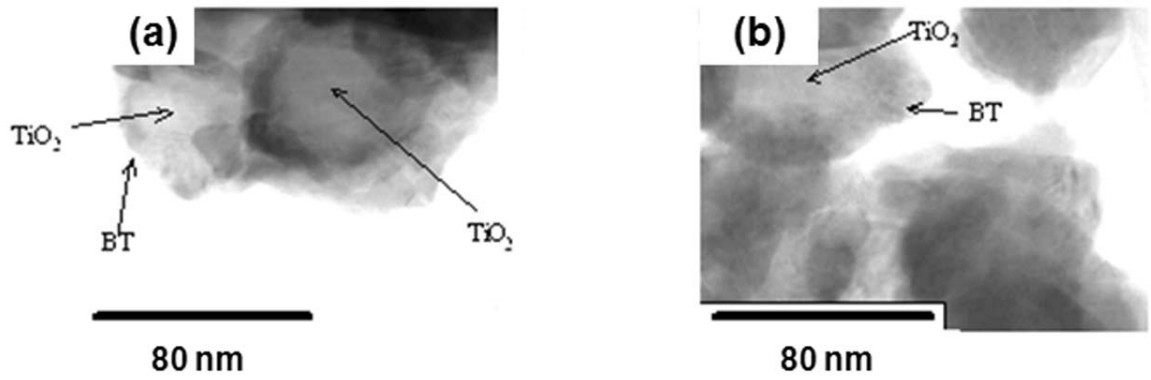

Figure 9. Grain morphology of barium titanate calcined at 700°C from: (a) intact mixture and (b) the mixture milled with 1.5 wt.% glycine for 1 h

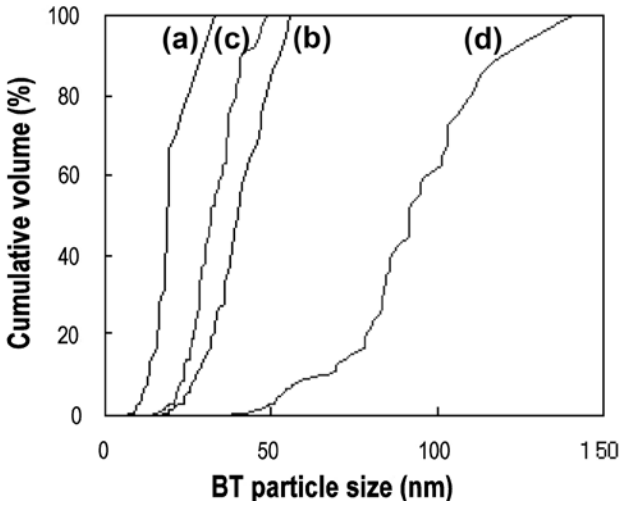

Figure 10. Particle size distribution of barium carbonate calcined from: (a)(b) intact mixture and (c)(d) the mixture milled with 1.5 wt.% glycine for 1 h, at (a)(c) 700°C and (b)(d) 790°C

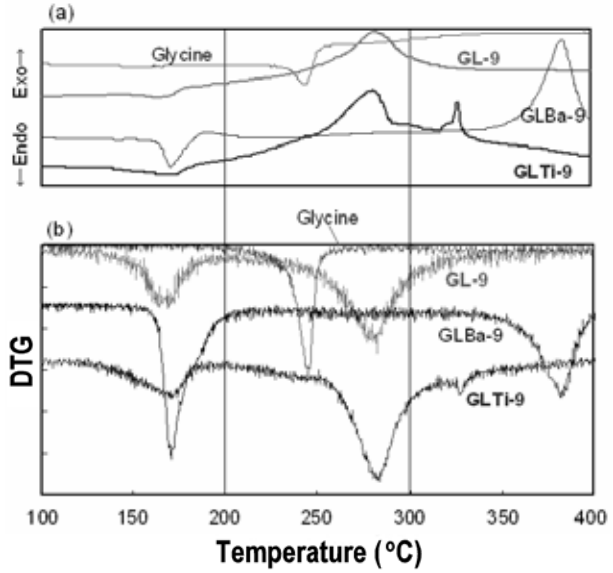

Figure 11. DTA curves (upper curves) and DTG curves (lower curves) of the samples with glycine addition of 9 wt.% to the mixture, $BaCO_3$ + TiO_2 (GL-9), to $BaCO_3$ (GL Ba-9) and to TiO_2 (GL Ti-9)

organic species. Particularly noteworthy is the persistence of the 48% of the organic species up to 384°C. Stepwise weight loss indicates decomposition of GLY, leaving a fraction with direct coordination to the inorganic substrates. It is important to note that multimodal DTG peak suggests the different mode of coordination of GLY to Ba and Ti.

Glycine can coordinate to metallic species by the lone pair electrons either of oxygen or nitrogen. In the case of amino acids to TiO_2, N-coordination is suggested based on the analyses of ESR [29]. This was also inferred in Chapter 2 with respect to mechanochemical anion substitution. We may not exclude bridging coordination of glycine to both Ba and Ti, although we do not have direct evidences for the time being.

Interaction between GLY and reactants was further examined by XPS analysis carried out *in situ* by varying the temperature. As shown in Fig. 12, O1s signals from the mixture without GLY (GL-0) comprise oxygen bound to Ba and Ti. Both of these peaks shift by changing the temperature. We also observed similar changes with temperature for other XPS peaks. The chemical shifts of $Ba3d_{5/2}$ and $Ti2p_{3/2}$ are plotted as a function of temperature in Fig. 13. We observe the plateau at temperatures between 300°C and 600°C for sample GL-0. A plateau was observed for the sample with 9 wt.% GLY (GL-9) at much lower temperatures, i.e. from the room temperature to 300°C, together with a second one at the temperature range similar to that of GL-0. The latter plateau, common to GL-0 and GL-9 is most probably attributed to the change from $BaCO_3$ to $BaTiO_3$. No change similar to former, i.e. at very low temperature, was observed on $O1s_{CO3}$ (not shown). From these observations, we suspect that GLY adsorbs preferentially on Ba side to change the bonding state between Ba^{2+} and CO_3^{2-}, even at room temperature, to ease the decomposition of $BaCO_3$.

Changes in the peak shift of $Ti2p_{3/2}$ are slightly different from those of $Ba3d_{5/2}$. The plateau appeared at a temperature range between 400°C and 600°C for GL-0,

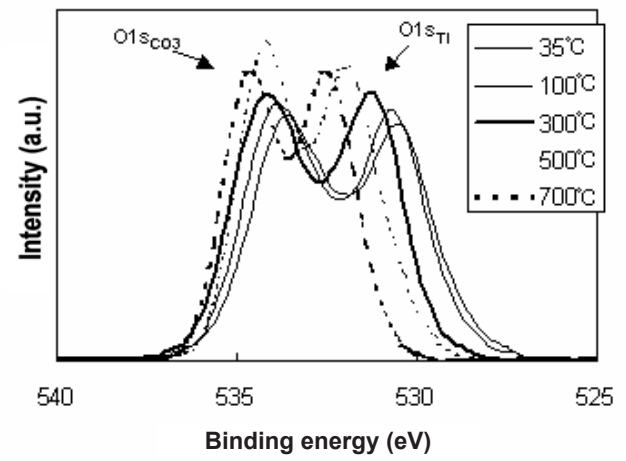

Figure 12. High-temperature XPS spectra of O1s of $BaCO_3$ and TiO_2 mixture after heating at respective temperatures

while between 200°C and 400°C for GL-9. These changes are in line with those for $O1s_{Ti}$ (not shown). This is an indication of the positive effect of GLY upon heating to promote the reaction toward $BaTiO_3$. An apparent change of $Ti2p_{3/2}$ are lower temperatures than that of $Ba3d_{5/2}$ may be corresponding to the microscopic observation shown in Fig. 9, where we observed apparent coverage of the newly formed $BaTiO_3$ around the TiO_2 particles. All these *in situ* XPS results consistently suggest that (1) GLY adsorbs at room temperature to Ba to promote the decomposition of $BaCO_3$, and (2) GLY serves as a reaction promoter upon heating to change the chemical states of TiO_2. Both of these effects serve to decrease the reaction temperature toward $BaTiO_3$.

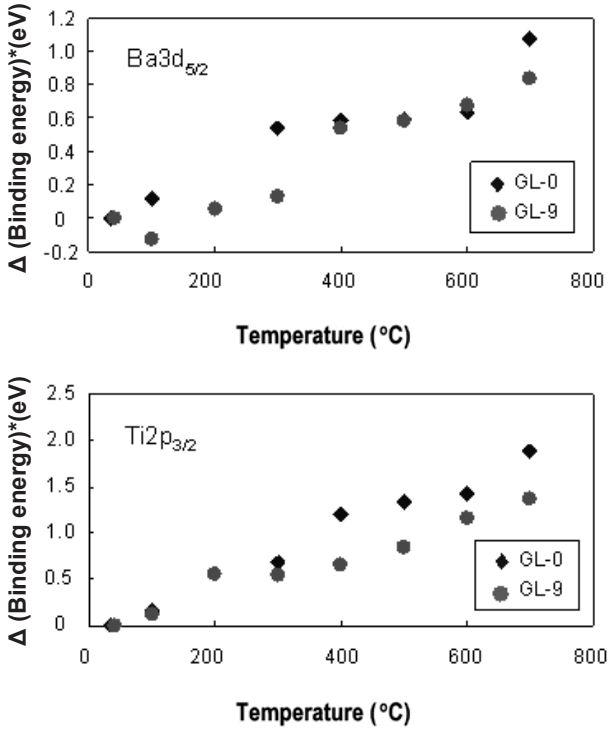

Figure 13. Change in the *in situ* XPS signals, $Ba3d_{5/2}$ and $Ti2p_{3/2}$, with temperature. GL-0: without glycine, GL-9: with 9 wt.% glycine

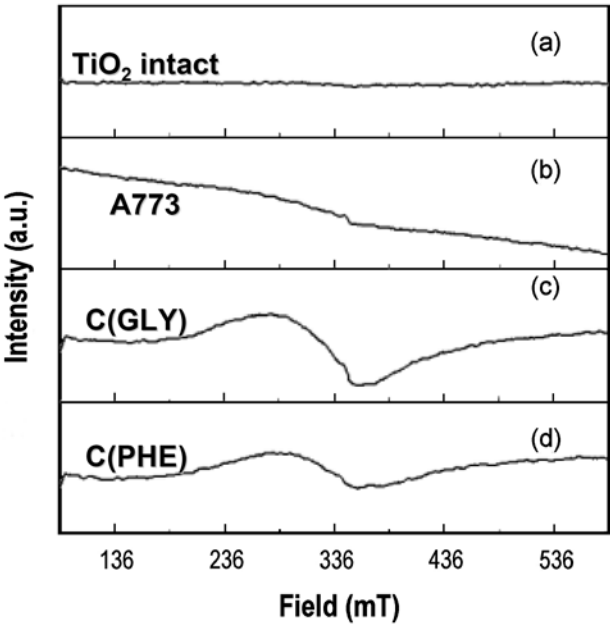

Figure 14. ESR spectra obtained at microwave frequency 9.40GHz ~ 9.45GHz, modulation width 0.32 mT. (a) TiO_2 intact, (b) intermediated obtained by calcining the stoichiometric mixture at 500°C, (c) and (d) $Li_4Ti_5O_{12}$ after calcination at 700°C starting from the intermediated milled with glycine (c) and phenylalanine (d).

3.6 Effects of OC on the phase pure synthesis of $Li_4Ti_5O_{12}$ nanoparticles

The author's group recently proposed a novel synthetic method of fine particles of highly pure $Li_4Ti_5O_{12}$ with their particle size as small as 70 nm [30]. When a stoichiometric mixture of $CH_3COOLi{\cdot}2H_2O$ and anatase fine particles of ca 50 nm was calcined at 500°C to obtain an intermediate, comprising Li_2TiO_3 and unreacted titania. The spirit of the method is to mechanically activate the intermediate with simultaneous addition of some amino acids, including GLY, alanine (ALA) or L-phenylalanine (PHE).

When we used ALA or PHE as an additive, microscopically determined average particle size of $Li_4Ti_5O_{12}$ was 70 nm ± 10 nm. Mechanisms and significance of the present two-step calcination with mechanical activation and addition of an amino acid to the intermediate were basically attributed to the favourable change in the chemical states of the reactants, among others titania. Diffuse reflectance spectra exhibited changes similar to those displayed in Chapter 2, Fig. 1. Activation of the reaction mixture was also demonstrated by the appearance of an ESR signal, as shown in Fig. 14.

The success of the present synthesis may also be associated with the topotactic nature of transformation between two layer-structured species, Li_2TiO_3 and

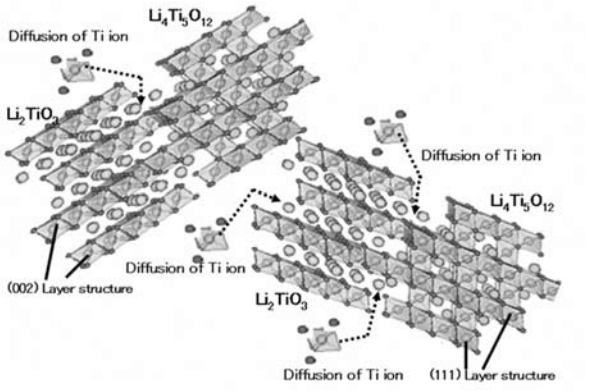

Figure 15. Scheme of a speculative reaction mechanism of $Li_4Ti_5O_{12}$ formation from the intermediate mixture, $Li_2TiO_3 + TiO_2$

$Li_4Ti_5O_{12}$. Instead of generally believed scheme of the diffusion of Li^+, migration of titanium ions into Li_2TiO_3 is not to be excluded, as schematically illustrated in Fig. 15, due to destabilization of TiO_6 units by the coordination of OC, together with the imperfect layer structure comprising the mixture of Li_2TiO_3 and $Li_4Ti_5O_{12}$.

IV. Concluding remarks

Merits of using OC for the syntheses of electroceramic materials via a solid state route can be divided into several components, i.e. acceleration of decomposition of a metal carbonate as a part to the reaction mixture to liberate diffusion species at temperatures lower than usual, and substitution of oxygen with nitrogen with simultaneous introduction of oxygen vacancies.

Intimate mixing of the reaction mixture with OCs coupled with mechanochemical treatments turned out to be quite promising to obtain phase pure perovskites with its average particle size below 200 nm. In the case of barium titanate (BT), its tetragonality was maintained as close to that of BT single crystal as possible. The same principle works in the case of synthesizing lithium titanate, $Li_4Ti_5O_{12}$, when OCs are added to the intermediate, Li_2TiO_3.

It is to be emphasized that organic substances mentioned in the present feature article could survive up to much higher temperatures than usual, because of the strong interaction with metal oxides, even when they have partially decomposed, maintaining their there effects up to the temperatures of calcination.

Acknowledgment: The cooperation under the COST 539 Action is highly acknowledged. The authors thank Dr. P. Bowen of EPFL for his valuable discussion, and Mr. H. Oguchi and Mr. R. Yanagawa for their experimental cooperation. The case study in Chapter 2 was mostly carried out in T.U. Braunschweig, supported by the Alexander von Humboldt foundation, with kind helps by Prof. K.D. Becker and his coworkers.

References

1. E. Boldyreva, "High-pressure studies of the anisotropy of structural distortion of molecular crystals", *J. Molec. Structure*, **647** (2003) 159–179.
2. E. Boldyreva, "High-pressure studies of the hydrogen bond networks in molecular crystals", *J. Molec. Structure*, **700** (2004) 151–155.
3. P.A. Wood, J.J. McKinnon, S. Parsons, E. Pidcock, M. Spackman, "Analysis of the compression of molecular crystal structures using Hirshfeld surfaces", *Cryst. Eng. Comm*., **10** (2008) 368–376.
4. J. Li, K.J. Van Vliet, T. Zhu, S. Yip, S. Suresh, "Atomistic mechanisms governing elastic limit and incipient plasticity in crystals", *Nature*, **418** (2002) 307–310.
5. E. Jaramillo, T.D. Sewell, A. Strachan, "Atomic-level view of inelastic deformation in a shock loaded molecular crystal", *Phys. Rev. B – Cond. Matter Mater. Phys*., **76** (2007) 064112.
6. C.M. Reddy, K.A. Padmanabhan, G.R. Desiraju, "Structure - property correlations in bending and brittle organic crystals", *Cryst. Growth Design*, **6** (2006) 2720–2731.
7. E. Laukhina, R. Pfattner, L.R. Ferreras, S. Galli, M. Mas-Torrent, N. Masciocchi, V. Laukhin, C. Rovira, J. Veciana, "Ultrasensitive piezoresistive all-organic flexible thin films", *Adv. Mater.*, **22** (2010) 977–981.
8. P. Mercandelli, M. Moret, A. Sironi, "Molecular Mechanics in Crystalline Media", *Inorg. Chem*., **37** (1998) 2563–2569.
9. C.M. Reddy, K.A. Padmanabhan, G.R. Desiraju, "Structure-property correlations in bending and brittle organic crystals", *Crystal Growth Design*, **6** (2006) 2720–2731.
10. A.E. Whitten, P. Turner, W.T. Klooster, R.O. Piltz, M.A. Spackman, "Reassessment of large dipole moment enhancements in crystals: A detailed experimental and theoretical charge density analysis of 2-methyl-4-nitroaniline", *J. Phys. Chem.*, *A* **110** (2006) 8763–8776.
11. R. Hiraoka, M. Senna, "Rational chemical reactions from solid-states by autogenous fusion of quinone–phenol systems via charge transfer complex", *Chem. Eng. Res. Design*, **87** (2009) 97–101.
12. N. Tsuchiya, A. Tsukamoto, T. Ohshita, T. Isobe, M. Senna, N. Yoshioka, H. Inoue, "Stress-induced ligand field distribution and consequent multi-mode spin crossover in $Fe^{II}(phen)_2(NCS)_2$ and $Fe^{II}[HB(pz)_3]_2$", *Solid State Sci*., **3** (2001) 705–714.
13. T. Ohshita, D. Nakajima, A. Tsukamoto, N. Tsuchiya, T. Isobe, M. Senna, N. Yoshioka, H. Inoue, "Role of molecular strain on the solid-state synthesis of coordination compounds from iron(II) chloride tetrahydrate and 1,10-phenanthroline under mechanical stress", *Ann. Chim. Sci. Mater*., **27** (2002) 91–101.
14. M. Cournil, M. Soustelle, G. Thomas, "Solid-solid reactions, II: Mechanism of barium metatitanate synthesis", *Oxidation Met*., **13** (1979) 89–104.

15. F. Bondioli, A.B. Corradi, A.M. Ferrari, T. Manfredini, G.G. Pellacani, "Kinetic study of conventional solid-state synthesis of $BaTiO_3$ by in situ HT-XRD", *Mater. Sci. Forum,* **278-281** (1998) 379–383.
16. A. Brzozowski, J. Sanchez, M.S. Castro, "$BaCO_3$-TiO_2 solid state reaction - A kinetic study", *J. Mater. Syn. Proc*., **10** (2002) 1–5.
17. M. Senna, V. Sepelak, J.M. Shi, B. Bauer, K.D. Becker, A. Feldhoff, "Preparation and properties of anion-modified TiO_2 nanoparticles via a mechanochemical route with organic fine particles", *Proc. World Congress Particle Technology*, 2010 in Nürnberg, in print.
18. C. Di Valentin, E. Finazzi, G. Pacchioni, A. Selloni, S. Livraghi, M.C. Paganini, E. Giamello, "N-doped TiO_2: Theory and experiment", *Chem. Phys*., **339** (2007) 44–56.
19. S. Indris, R. Amade, P. Heitjans, M. Finger, A. Haeger, D. Hesse, W. Grünert, K.D. Becker, "Preparation by high-energy milling, characterization, and catalytic properties of nanocrystalline TiO_2", *J. Phys. Chem*., **B 109** (2005) 23274–23278.
20. S. Bégin-Colin, A. Gadalla, G. Le Caër, O. Humbert, F. Thomas, O. Barres, F. Villiéras, P. Gilliot, "On the origin of the decay of the photocatalytic activity of TiO_2 powders ground at high energy", *J. Phys. Chem*., **C 113** (2009) 16589–16602.
21. T. Müller, T. Großmann, H.-P. Abicht, "Nitrogen containing barium titanate: Preparation and characterisation", *J. Phys. Chem. Solid*, **70** (2009) 1093–1097.
22. D. Li, N. Ohashi, S. Hishita, T. Kolodiazhnyi, H. Haneda, "Origin of visible-light-driven photocatalysis: A comparative study on N/F-doped and N-F-codoped TiO_2 powders by means of experimental characterizations and theoretical calculations", *J. Solid State Chem*., **178** (2005) 3293–3302.
23. R. Yanagawa, C. Ando, H. Chazono, H. Kishi, M. Senna, "Well-crystallized tetragonal $BaTiO_3$ micro particles via a solid-state reaction preceded by agglomeration-free mechanical activation", *J. Am. Ceram. Soc*., **90** (2007) 809–814.
24. C. Ando, H. Kishi, H. Oguchi, M. Senna, "Effects of bovine serum albumin on the low temperature synthesis of barium titanate microparticles via a solid state roots", *J. Am. Ceram. Soc*., **89** (2006) 1709–1712.
25. H. Oguchi, C. Ando, H. Chazono, H. Kish, M. Senna, "Effects of glycine on the solid-state synthesis of barium titanate micro-particles with high tetragonality", *J. Phys. IV France*, **128** (2005) 33–39.
26. M. Valefi, C. Falamaki, T. Ebadzadeh, M.S. Hashjin, "New insights of the glycine-nitrate process for the synthesis of nano-crystalline 8YSZ", *J. Am. Ceram. Soc*., **90** (2007) 2008–2014.
27. C. Ando, T. Suzuki, Y. Mizuno, H. Kishi, S. Nakayama, M. Senna, "Evaluation of additive effects and homogeneity of the starting mixture on the nuclei-growth processes of barium titanate via a solid state route", *J. Mater. Sci*., **43** (2008) 6182–6192.
28. C. Ando, K. Tsuzuku, T. Kobayashi, H. Kishi, S. Kuroda, M. Senna, "Function of glycine during solid-state reaction toward well-crystallized fine particulate barium titanate", *J. Mater. Sci*.: *Mater. Electronics*, **20** (2009) 844–850.
29. S.K. Joung, T. Amemiya, M. Murabayashi, K. Itoh, "Mechanistic studies of the photocatalytic oxidation of trichloroethylene with visible-light-driven N-doped TiO_2 photocatalysts", *Chemistry - A Eur. J*., **12** (2006) 5526–5534.
30. E. Matsui, Y. Abe, M. Senna, A. Guerfi, K. Zaghib, "Solid state synthesis of pure phase 70 nm $Li_4Ti_5O_{12}$ particles by mechanically activating intermediates with amino acids", *J. Am. Ceram. Soc*., **91** (2008) 1522–1527.